Ferroelectricity and Phase Transitions in Monolayer Group-IV Monochalcogenides

Ruixiang Fei,[1] Wei Kang,[2,*] and Li Yang[1,†]
[1]Department of Physics and Institute of Materials Science and Engineering, Washington University in St. Louis, St. Louis, Missouri 63130, USA
[2]HEDPS, Center for Applied Physics and Technology, and College of Engineering, Peking University, Beijing 100871, China
(Received 4 April 2016; revised manuscript received 25 July 2016; published 23 August 2016)

Ferroelectricity usually fades away as materials are thinned down below a critical value. We reveal that the unique ionic-potential anharmonicity can induce spontaneous in-plane electrical polarization and ferroelectricity in monolayer group-IV monochalcogenides MX (M = Ge, Sn; X = S, Se). An effective Hamiltonian has been successfully extracted from the parametrized energy space, making it possible to study the ferroelectric phase transitions in a single-atom layer. The ferroelectricity in these materials is found to be robust and the corresponding Curie temperatures are higher than room temperature, making them promising for realizing ultrathin ferroelectric devices of broad interest. We further provide the phase diagram and predict other potentially two-dimensional ferroelectric materials.

DOI: 10.1103/PhysRevLett.117.097601

Ferroelectrics, particularly the thin-film form that is most commonly needed for modern devices, is plagued by a fundamental challenge: the depolarization field—an internal electric field that competes with and often destroys ferroelectricity [1–3]. As a result, the critical thickness in proper ferroelectric materials, such as perovskite ones, is limited between 12 and 24 Å [4–6]. New mechanisms such as hyperferroelectrics are proposed to keep the polarization even in a single layer of ABC hexagonal semiconductors [7], but these materials have yet to be synthesized. Layered van der Waals (vdW) materials may provide another way to overcome this challenge. For example, two-dimensional (2D) MoS_2 was predicted to be a potentially ferroelectric material [8]. However, its ferroelectric $1T$ structure is not thermally stable compared to the observed $2H$ phase.

Bulk SnSe, a high-performance thermoelectric material [9], exhibits giant anharmonic and anisotropic phonons [10–13], which are usually the signs of spontaneous symmetry breaking. In particular, monolayer structures of this MX (M = Ge, Sn; X = S, Se) family are predicted to own giant piezoelectricity [14,15] and, particularly, their electrical polarization displays a nonlinear response to applied strain [14]. All these clues motivate us to investigate if these materials are spontaneously polarized and ferroelectric. From the point of view of fabrication, ultrathin trilayers of these materials have been successfully fabricated [16], making the study of monolayers of immediate interest. Last, but not least, the relation between phase transitions and dimensionality has been a century-long topic [17,18]. Beyond intensive studies on bulk ferroelectric phase transitions [1,19–21], ferroelectric phase transitions in 2D materials and their critical phenomena are obviously of fundamental importance.

In this work, we show that MX (M = Ge, Sn; X = S, Se) monolayers are a new family of 2D ferroelectric vdW materials. Using first-principles calculations [22–28], we identify two degenerate structures exhibiting spontaneous in-plane polarization. Moreover, we build an effective Hamiltonian to investigate the phase transition via Monte Carlo (MC) simulations [22]. The calculated Curie temperatures (T_C) are above room temperature, making these materials promising for experiments and ultrathin ferroelectric devices. We further demonstrate that this 2D ferroelectric phase transition obeys the fourth-order Landau theory but with different critical exponents from those of the typical second-order phase transition [29]. Finally, we obtain the phase diagram of monolayer SnSe, showing that minor strain can dramatically tune T_C. By computing covalency and cophonicity metrics, we show the correlation between the ionic-covalent bonds with spontaneous polarization and Curie temperatures, which may give hope to the search for new 2D ferroelectric materials.

Bulk MX (M = Ge, Sn; X = S, Se) adopts a layered orthorhombic structure (space group $Pnma$) at room temperature, which is derived from a three-dimensional distortion of the NaCl structure (space group $Cmcm$) [9]. Their monolayer structures keep this symmetry [22,30], as shown in Fig. 1(a). From the side view, we define the angles θ_1 and θ_2 measured along the x (armchair) direction shown in Fig. 1(b), which describes the geometric distortion. When $\theta_1 = \theta_2 = 0$, the structure converts back to the nonpolar $Cmcm$ (phase A) with the inversion symmetry, which is actually the structure of the crystalline insulator materials, SnTe and PbTe, etc. [22,31].

For monolayer MXs, there are two stable structures which are related by a spatial inversion, characterized by having both θ_1 and θ_2 positive or both negative. These structures, labeled by phases B and B', are shown in Fig. 1(b). Taking monolayer SnSe as an example, the free-energy contour obtained using first-principles

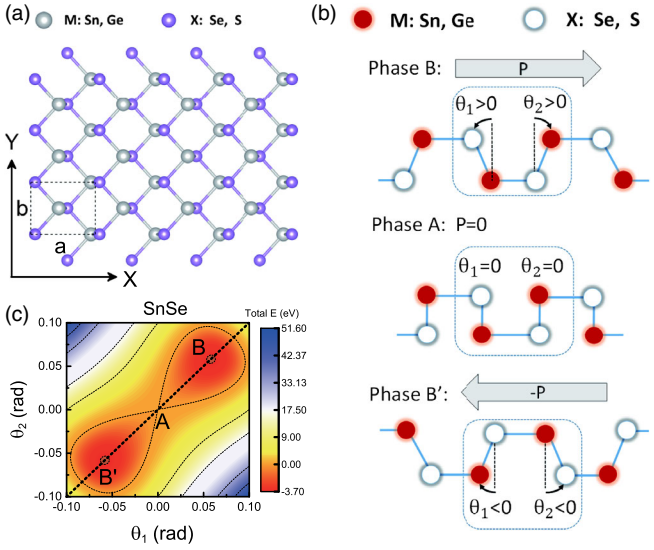

FIG. 1. (a) Top view of the structure of monolayer group-IV monochalcogenides. The black line rectangle is the first Brillouin zone, a is the lattice constant along the armchair direction (x), and b is that along the zigzag direction (y). (b) The schematic side views of the two distorted degenerate polar structures (B and B') and the high symmetry nonpolar phase (A). (c) The free-energy contour plot of monolayer SnSe according to the tilting angles (θ_1 and θ_2). The phases A, B, and B' are marked.

calculations is presented in Fig. 1(c), which confirms these stable structures (B and B') are connected through a saddle point (A). This anharmonic double-well potential strongly hints the existence of ferroelectricity.

Importantly, both B and B' structures are noncentrosymmetric polar, and they can be transformed into another by a spatial inversion. Therefore, if there is a polarization (P) in the B phase, that of the B' phase must be the inverse ($-P$). Our Berry-phase calculation based on density functional theory (DFT) confirms this symmetry analysis: these two stable structures (B and B') have significant spontaneous polarization with opposite polarizing directions. The spontaneous polarization at zero temperature (P_s) are listed in Table I. If we estimate the thickness of each layer to be 0.5 nm [9], their average bulk values of the polarization are around 0.3–1.0 C/m^2, which are similar to those of traditional ferroelectric materials such as $BaTiO_3$ and Lead zirconate titanate (PZT) [21,32,33].

TABLE I. The ground-state free energy (potential barrier) E_G (meV), the spontaneous polarization P_s (10^{-10} C/m) at zero temperature, and fitted parameters in Eq. (1). A, B, and C are used to describe the double-well potential. D is the constant representing the mean-field approximation interaction between the nearest neighbors.

Material	E_G	P_s	A	B	C	D
SnSe	−3.758	1.51	−5.785	1.705	0.317	10.16
SnS	−38.30	2.62	−19.127	1.053	0.275	8.49
GeSe	−111.99	3.67	−15.869	−3.540	0.378	9.74
GeS	−580.77	5.06	−37.822	−5.422	0.280	10.59

Soft optical modes correspond to displacive instabilities and have been assigned to be the driving mechanism for spontaneous symmetry breaking in bulk ferroelectrics [34]. As temperature decreases below T_C, the frequency of the soft mode will evolve to be imaginary, driving the high-symmetry structure to a symmetry-broken phase. We have observed the similar phenomenon. For example, in monolayer SnSe, we plot the phonon dispersions for both the nonpolar phase A and polar phase B [Figs. 2(a) and 2(b)]. Clearly there is an imaginary, soft optical mode (λ) presenting, and it is corresponding to the symmetry breaking below T_C.

Beyond the calculation of ferroelectricity at zero temperature, a more fundamental question is the corresponding ferroelectric phase transition, which has been intensively studied for decades in bulk materials [1,20,34–38]. This is an open question for monolayer monochalcogenides because of their 2D nature. Dimensionality is a key factor deciding phase transitions. In particular, lower dimensionality usually enhances fluctuations, decreasing or even diminishing phase transitions. Therefore, even with a finite configurational potential barrier [Fig. 1(c)], it is unknown if such a ferroelectric order can survive (robust) at finite temperature in 2D materials. This is also crucial for potential devices working at room temperature. In the following, we build a quantitative approach to study the 2D ferroelectric phase transition beyond zero-temperature DFT calculations.

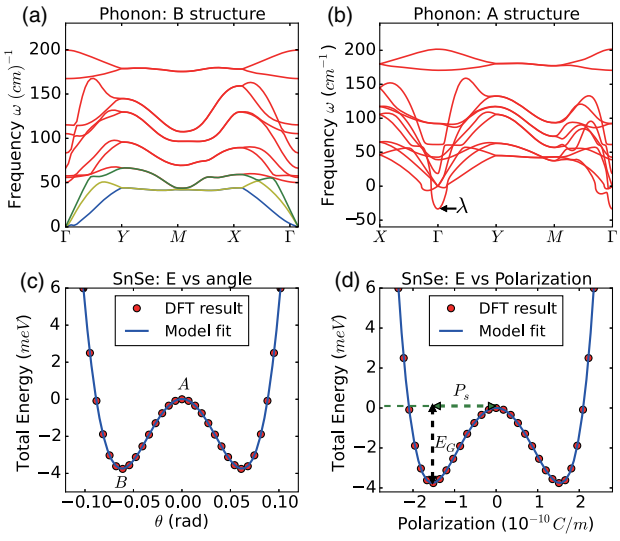

FIG. 2. (a) and (b) Phonon spectra of the structures A and B of monolayer SnSe, respectively. (c) Double-well potential of monolayer SnSe. Red points are the DFT-calculated total energy and the blue line is from the model. (d) Double-well potential vs polarization. E_G is the ground-state energy (potential barrier) and P_s is the spontaneous polarization.

Although the aforementioned soft optical mode is the driving mechanism for the ferroelectric phase transition, it is not easy to describe these modes at finite temperature. Moreover, techniques for treating higher-order anharmonic phonons, which are crucial to induce phase transitions, are limited. One approximation of investigating the imaginary modes is to employ the so-called *renormalization scheme* to calculate the effective harmonic frequencies at finite temperature [11]. However, in that scheme, it is hard to distinguish different dimensionalities, which is the essential feature for 2D ferroelectric phase transition.

Alternatively, we describe our system by the Landau theory. The polarization P is the order parameter. Then we need to map the two-component (θ_1, θ_2) free-energy surface [Fig. 1(c)] to a function of the order parameter P. However, a brute-force 2D mapping will result in formidable simulation. Fortunately, we observe that due to the steep gradient of the energy surface along the perpendicular direction to the dashed diagonal line in Fig. 1(c), the structure prefers to stay as the so-called *angle-covariant* phase ($\theta_1 = \theta_2$), marked by the dashed line in Fig. 1(c) (details in Secs. IV and V of the Supplemental Material [22]). This makes it possible to only consider a 1D subset of configurations and greatly simplifies the parameter space.

In Fig. 2(c), we show the energy along this angle-covariant line, $\theta_1 = \theta_2 = \theta$, for monolayer SnSe. Its double-well shape suggests the known form of the ϕ^4 potential, which has been widely used to study bulk ferroelectric materials [21,39]. By calculating the polarization for each value of θ, we can connect the free energy E to the polarization P.

The potential energy is expressed in the Landau-Ginzburg expansion

$$E = \sum_i \frac{A}{2}(P_i^2) + \frac{B}{4}(P_i^4) + \frac{C}{6}(P_i^6) + \frac{D}{2}\sum_{\langle i,j\rangle}(P_i - P_j)^2, \qquad (1)$$

which can be viewed as the Taylor series of local structural distortions with a certain polarization defined at each cell P_i. As shown in Fig. 2(d), the first three terms are associated with the energy contribution from the local modes up to the sixth order and they well describe the anharmonic double-well potential. The last term captures the coupling between the nearest local modes and includes the 2D geometry that is crucial for differentiating this work from previous bulk studies. Compared with the results of mean-field theory within the nearest-neighbor approximation [Fig. 3(a)], the first-principles calculations of supercells show that the coupling is harmonic, confirming the validity of keeping the second-order interactions in Eq. (1). The values of the parameters A–D are listed in Table I. Interestingly, the value for D, describing the average dipole-dipole interaction, is almost the same across these four materials. This is from the similar local structures of these materials.

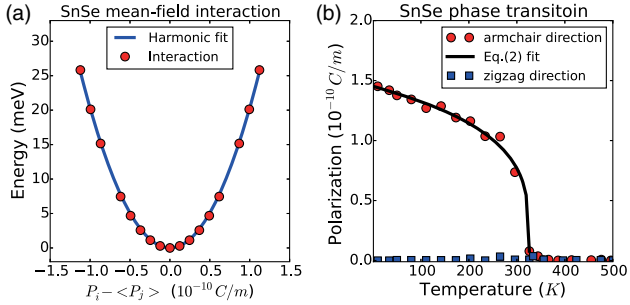

FIG. 3. (a) The dipole-dipole interaction of monolayer SnSe by using mean-field theory. The red points are the DFT-calculated total energy of different $P_i - \langle P_j \rangle$. The blue line is fitted by the harmonic approximation. (b) Temperature dependence of polarization obtained from MC simulations of monolayer SnSe.

With this effective Hamiltonian and parameters, we can employ the MC simulation to investigate the phase transition. In Fig. 3(b), take monolayer SnSe as an example, we show there is an abrupt transition at $T_C \approx 325$ K. To obtain the critical exponents and understand universal critical phenomena, we employ a fitting procedure that assumes a heuristic form for $P(T)$:

$$P(T) = \begin{cases} \mu(T_C - T)^{\delta} & T < T_C \\ 0 & T > T_C, \end{cases} \qquad (2)$$

where T_C is the Curie temperature, δ is the critical exponent, and μ is a constant. These fitted results of monolayer MX are summarized in Table II. The critical exponents are around 0.25 and 0.35, which are significantly below the ideal value (0.5) based on the 2D ferromagnetic Ising model [29]. This is similar to the conclusion from bulk ferroelectric perovskites [21]. In this sense, our study is still not enough to identify the type of this phase transition and it is an extremely interesting question for future studies by further observing the hysteresis in heating and cooling [40].

In Table II, the Curie temperature T_C of monolayer GeS and GeSe are rather large; this is consistent with their higher configurational energy barriers (E_G in Table I), indicating that GeSe and GeS have strong ferroelectric instability. On the other hand, the smaller T_C of monolayer SnSe and SnS show they have weak ferroelectric instability, which can be easily tuned by external field or strain. This is

TABLE II. The Curie temperature (T_C) and critical exponents in Eq. (2).

Material	T_C (K)	μ	δ
SnSe	326	0.34	0.25
SnS	1200	0.21	0.35
GeSe	2300	0.48	0.26
GeS	6400	0.75	0.22

also consistent with our previous work showing a nonlinear polarization response in strained SnSe and SnS [14].

It is important to point out that the Curie temperature T_C cannot be simply estimated by the configurational energy barriers. For example, the barrier of the double-well potential $|E_G|$ of SnSe (3.758 meV) is much smaller than its $k_B T_C$ (28.02 meV). This can be explained by the fourth-order Landau theory, which has been used to understand the ferroelectricity of perovskites [41]. In this scheme, the free energy can be written as

$$F = \alpha(T - T_C)P^2 + \beta P^4, \tag{3}$$

with $\alpha,\beta > 0$. The equilibrium polarization is given by $dF/dP = 0$, resulting in the Curie temperature

$$T_C = \frac{2\beta}{\alpha} {P_s}^2. \tag{4}$$

Excitingly, we fit the calculated spontaneous polarization of monolayer SnSe and find $T_C \sim P_s^2$, which perfectly matches the Landau theory, similar to traditional perovskite ferroelectric materials [21,42]. More precisely, the coefficient $2\beta/\alpha$ is about 11.09 meV/$(10^{-10}$ C/m$)^2$, which is very close to the interaction constant D of monolayer SnSe listed in Table I. Therefore, a material with weak instability may nevertheless display relatively high T_C determined by high values of dipole-dipole coupling D and the spontaneous polarization P_s. This may be particularly interesting for suspended 2D ferroelectric materials because the surrounding vacuum cannot efficiently screen the dipole-dipole interaction, enhancing the coefficient in Eq. (4) and further increasing the Curie temperature.

Phase diagrams are particularly important for completely describing ferroelectricity in monolayers because the 2D materials are easily affected by substrates [43,44], fabrications, and temperature [45]. For monolayers, it is hard to define the in-plane pressure. Equivalently, we provide a phase diagram, in which we vary the two orthogonal lattice constants (a and b) that can be related to strain and calculate the corresponding Curie temperature; see Sec. V of the Supplemental Material [22]. As an example, the phase diagram of monolayer SnSe is presented in Fig. 4(b). Interestingly, the ferroelectric transition temperature could be tuned in a wide range (a few hundred Kelvins) by very small strain (within $\pm 1\%$) along the x (armchair) direction. This widely tunable range, without insulator-metal transition [45], suggests potential deviations for experimental measurements and it is also promising for the engineering ferroelectricity.

Understanding the correlation between structure distortions, spontaneous polarization, and the chemical bonding nature is important for predicting new ferroelectric materials. Here we investigate covalency and cophonicity metrics (more details in Sec. VII of Supplemental Material [22]) proposed by Cammarata *et al.* [46,47], which are useful

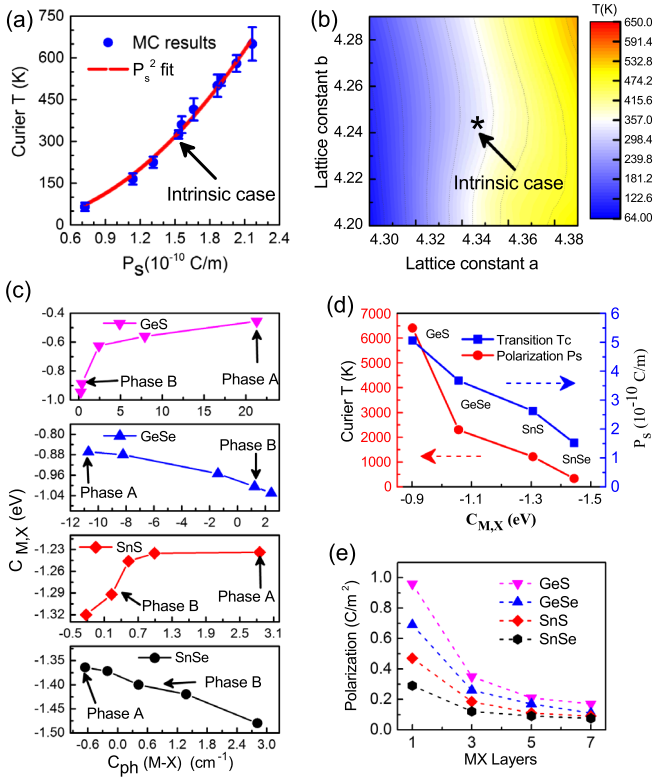

FIG. 4. (a) Curie temperature vs the spontaneous polarization. The blue points and error bars are MC simulations and the red line is the fitted result using the model function in Eq. (4). (b) Phase diagram of monolayer SnSe under strain. (c) M-X bond covalency $C_{M,X}$ vs cophonicity $C_{\mathrm{ph}}(M\text{–}X)$ with different covariant angles. (d) Curie T_C and spontaneous polarization P_s vs M-X bond covalency $C_{M,X}$. (e) Polarization at zero temperature vs the layer number of MXs.

tools for analyzing structural distortions and ferroelectricity. We show the M-X bond covalency $C_{M,X}$ vs the MX cophonicity $C_{\mathrm{ph}}(M\text{–}X)$. in Fig. 4(c). Although the covalencies have different monotonic behaviors with respect to the cophonicity $C_{\mathrm{ph}}(M\text{–}X)$, the cophonicity approaches a perfect cophonocity $[C_{\mathrm{ph}}(M\text{–}X) = 0]$ when the phase is varied from the structure A to the more stable and polar structure B. Thus cophonicity may be a useful quantity for predicting stable ferroelectric structures. In Fig. 4(d), we show the covalency $C_{M,X}$ according to the polarization and the critical temperature. Interestingly, we find that the more ionic material (smaller $C_{M,X}$) has smaller P_s and lower T_C. This rule is consistent with the fact that the heavy compound SnTe (ionic NaCl type structure) is not a spontaneous polarization material. According to this rule, we expect that the less covalent MX, such as the monolayer SiS [48] and $As_{1-x}P_x$ compound [49,50] may have higher spontaneous polarization and Curie temperatures.

Finally, beyond monolayers, it is necessary to mention few-layer monochalcogenides, given the fact that trilayer SnSe have been fabricated [16]. Because of the restored inversion symmetry, the polarization of even-number-layer

MXs is always zero. In Fig. 4(d) we show the spontaneous polarization of odd-number-layer MXs, in which the 2D polarization (C/m) is renormalized to bulk values (C/m^2). Interestingly, although polarization of the odd-number layers MXs decays with the increasing thickness, the P_s of five layers SnSe is still around 0.08 C/m^2 ($= 8\ \mu C/cm^2$), which is comparable to those of paraelectric barium titanate [51] and $BaTiO_3$ multiferroic nanostructures [52]. Thus, it is possible to observe the ferroelectricity in currently available few-layer monochalcogenides [16].

In conclusion, we predict that monolayer–odd-number-layer group-IV monochalcogenides are ferroelectric materials with in-plane spontaneous polarization. The Curie temperatures are significantly higher than their configurational energy barriers between their degenerated ground-state structures. These properties indicate that monolayer MXs are robust ferroelectric materials, which could be useful for devices. The revealed mechanism of the ferroelectric phase transition, explained by the Landau theory, takes us closer to understand the universal critical properties of 2D materials. Furthermore, the widely tunable Curie temperature of these monolayers under small strain gives more freedom for engineering ferroelectric devices. Finally, based on our covalency analysis, new materials, such as SiS [48] and $As_{1-x}P_x$, are predicted to be higher P_s and T_C.

We acknowledge fruitful discussions with Wenshen Song, Vy Tran, and Shiyuan Gao. We are supported by the National Science Foundation (NSF) CAREER Grant No. DMR-1455346, NSF EFRI-2DARE-1542815, and the International Center for Advanced Renewable Energy & Sustainability (I-CARES). The computational resources have been provided by the Stampede of Teragrid at the Texas Advanced Computing Center (TACC) through XSEDE.

Note added.—Recently, we became aware of theoretical studies by Hanakata *et al.* [53] and Wu and Zeng [54], which show ferroelasticity and ferroelectricity of these 2D materials.

*weikang@pku.edu.cn
†lyang@physics.wustl.edu

[1] I. P. Batra, P. Wurfel, and B. D. Silverman, Phys. Rev. Lett. **30**, 384 (1973).
[2] W. Zhong, R. D. King-Smith, and D. Vanderbilt, Phys. Rev. Lett. **72**, 3618 (1994).
[3] M. Dawber, K. M. Rabe, and J. F. Scott, Rev. Mod. Phys. **77**, 1083 (2005).
[4] J. Junquera and P. Ghosez, Nature (London) **422**, 506 (2003).
[5] D. D. Fong, G. B. Stephenson, S. K. Streiffer, J. A. Eastman, O. Auciello, P. H. Fuoss, and C. Thompson, Science **304**, 1650 (2004).
[6] C. Ahn, K. Rabe, and J.-M. Triscone, Science **303**, 488 (2004).
[7] K. F. Garrity, K. M. Rabe, and D. Vanderbilt, Phys. Rev. Lett. **112**, 127601 (2014).
[8] S. N. Shirodkar and U. V. Waghmare, Phys. Rev. Lett. **112**, 157601 (2014).
[9] L.-D. Zhao, S.-H. Lo, Y. Zhang, H. Sun, G. Tan, C. Uher, C. Wolverton, V. P. Dravid, and M. G. Kanatzidis, Nature (London) **508**, 373 (2014).
[10] C. Li, J. Hong, A. May, D. Bansal, S. Chi, T. Hong, G. Ehlers, and O. Delaire, Nat. Phys. **11**, 1063 (2015).
[11] J. M. Skelton, L. A. Burton, S. C. Parker, A. Walsh, C.-E. Kim, A. Soon, J. Buckeridge, A. A. Sokol, C. R. A. Catlow, A. Togo, and I. Tanaka, Phys. Rev. Lett. **117**, 075502 (2016).
[12] J. Carrete, N. Mingo, and S. Curtarolo, Appl. Phys. Lett. **105**, 101907 (2014).
[13] L.-D. Zhao, G. Tan, S. Hao, J. He, Y. Pei, H. Chi, H. Wang, S. Gong, H. Xu, V. P. Dravid, C. Uher, G. J. Snyder, C. Wolverton, and M. G. Kanatzidis, Science **351**, 141 (2016).
[14] R. Fei, W. Li, J. Li, and L. Yang, Appl. Phys. Lett. **107**, 173104 (2015).
[15] L. C. Gomes, A. Carvalho, and A. H. Castro Neto, Phys. Rev. B **92**, 214103 (2015).
[16] L. Li, Z. Chen, Y. Hu, X. Wang, T. Zhang, W. Chen, and Q. Wang, J. Am. Chem. Soc. **135**, 1213 (2013).
[17] F. J. Dyson, Commun. Math. Phys. **12**, 91 (1969).
[18] H. E. Stanley and T. A. Kaplan, Phys. Rev. Lett. **17**, 913 (1966).
[19] S. Chattopadhyay, P. Ayyub, V. R. Palkar, and M. Multani, Phys. Rev. B **52**, 13177 (1995).
[20] W. Zhong, D. Vanderbilt, and K. M. Rabe, Phys. Rev. Lett. **73**, 1861 (1994).
[21] J. C. Wojdeł and J. Íñiguez, Phys. Rev. B **90**, 014105 (2014).
[22] See Supplemental Material at http://link.aps.org/supplemental/10.1103/PhysRevLett.117.097601, which includes Refs. [23]. We show the computational method details in Sec. 1, lattice constants of the stable phase monolayer MX (Sec. II), the *Pnma* structure and *Cmcm* structure of monolayer group-IV monochalcogenides (Sec. III), explanation of using the angle-covariant model (Sec. IV), the connection between the Angle Model and Landau-Ginzburg theory (Sec. V), the calculation details of the phase diagram of monolayer SnSe (Sec. VI), and the covalency and cophonicity calculation details of MXs (Sec. VII).
[23] S. Grimme, J. Comput. Chem. **27**, 1787 (2006).
[24] G. Kresse and D. Joubert, Phys. Rev. B **59**, 1758 (1999).
[25] J. P. Perdew, K. Burke, and M. Ernzerhof, Phys. Rev. Lett. **77**, 3865 (1996).
[26] A. Togo, F. Oba, and I. Tanaka, Phys. Rev. B **78**, 134106 (2008).
[27] R. D. King-Smith and D. Vanderbilt, Phys. Rev. B **47**, 1651 (1993).
[28] R. Resta, Rev. Mod. Phys. **66**, 899 (1994).
[29] M. E. Newman, G. T. Barkema, and M. Newman, *Monte Carlo Methods in Statistical Physics* (Clarendon Press, Oxford, 1999), Vol. 13.
[30] G. Shi and E. Kioupakis, Nano Lett. **15**, 6926 (2015).
[31] J. Liu, X. Qian, and L. Fu, Nano Lett. **15**, 2657 (2015).
[32] K. J. Choi, M. Biegalski, Y. L. Li, A. Sharan, J. Schubert, R. Uecker, P. Reiche, Y. B. Chen, X. Q. Pan, V. Gopalan,

L.-Q. Chen, D. G. Schlom, and C. B. Eom, Science **306**, 1005 (2004).
[33] X. Wu, K. M. Rabe, and D. Vanderbilt, Phys. Rev. B **83**, 020104 (2011).
[34] P. A. Fleury, J. F. Scott, and J. M. Worlock, Phys. Rev. Lett. **21**, 16 (1968).
[35] U. V. Waghmare and K. M. Rabe, Phys. Rev. B **55**, 6161 (1997).
[36] Z. Wu and R. E. Cohen, Phys. Rev. Lett. **95**, 037601 (2005).
[37] J. Paul, T. Nishimatsu, Y. Kawazoe, and U. V. Waghmare, Phys. Rev. Lett. **99**, 077601 (2007).
[38] I. C. Infante, J. Juraszek, S. Fusil, B. Dupé, P. Gemeiner, O. Diéguez, F. Pailloux, S. Jouen, E. Jacquet, G. Geneste, J. Pacaud, J. Íñiguez, L. Bellaiche, A. Barthélémy, B. Dkhil, and M. Bibes, Phys. Rev. Lett. **107**, 237601 (2011).
[39] A. D. Bruce, Adv. Phys. **29**, 111 (1980).
[40] W. Zhong, D. Vanderbilt, and K. M. Rabe, Phys. Rev. B **52**, 6301 (1995).
[41] I. Grinberg and A. M. Rappe, Phys. Rev. B **70**, 220101 (2004).
[42] S. C. Abrahams, S. K. Kurtz, and P. B. Jamieson, Phys. Rev. **172**, 551 (1968).
[43] M. Neek-Amal and F. Peeters, Appl. Phys. Lett. **104**, 173106 (2014).
[44] A. Mogulkoc, Y. Mogulkoc, A. N. Rudenko, and M. I. Katsnelson, Phys. Rev. B **93**, 085417 (2016).
[45] M. Mehboudi, B. M. Fregoso, Y. Yang, W. Zhu, A. van der Zande, J. Ferrer, L. Bellaiche, P. Kumar, and S. Barraza-Lopez, arXiv:1603.03748.
[46] A. Cammarata and J. M. Rondinelli, J. Chem. Phys. **141**, 114704 (2014).
[47] A. Cammarata and T. Polcar, Inorg. Chem. **54**, 5739 (2015).
[48] J. Yang, Y. Zhang, W.-J. Yin, X. Gong, B. I. Yakobson, and S.-H. Wei, Nano Lett. **16**, 1110 (2016).
[49] Z. Zhu, J. Guan, and D. Tománek, Nano Lett. **15**, 6042 (2015).
[50] B. Liu, M. Köpf, A. N. Abbas, X. Wang, Q. Guo, Y. Jia, F. Xia, R. Weihrich, F. Bachhuber, F. Pielnhofer *et al.*, Adv. Mater. **27**, 4423 (2015).
[51] J. Narvaez, S. Saremi, J. Hong, M. Stengel, and G. Catalan, Phys. Rev. Lett. **115**, 037601 (2015).
[52] C.-W. Nan, G. Liu, Y. Lin, and H. Chen, Phys. Rev. Lett. **94**, 197203 (2005).
[53] P. Z. Hanakata, A. Carvalho, D. K. Campbell, and H. S. Park, Phys. Rev. B **94**, 035304 (2016).
[54] M. Wu and X. C. Zeng, Nano Lett. **16**, 3236 (2016).